

RESEARCH

Open Access



USP2 reversed cisplatin resistance through p53-mediated ferroptosis in NSCLC

Yanmei Gong¹, Ruichao Li¹, Rui Zhang¹ and Li Jia^{1*}

Abstract

Background It has demonstrated the indispensable role of ferroptosis in conferring cisplatin resistance in non-small cell lung cancer (NSCLC), as well as the involvement of ubiquitin-specific protease (USP) in regulating ferroptosis. This paper aspired to the mechanism of USP2 and ferroptosis on NSCLC cisplatin resistance.

Methods Ubiquitin-specific protease mRNA expression, was detected through RT-qPCR. In vitro functional assays assessed the effects of USP2 overexpression on DDP resistance, cell proliferation capability, and ferroptosis markers in A549/DDP and H1299/DDP cells. Ubiquitination assays evaluated the ubiquitination levels of p53 following USP2 overexpression. Co-immunoprecipitation (Co-IP) assays confirmed the binding relationship between USP2 and p53. In vivo experiments in mice explored the specific role of the USP2-p53 axis in a xenograft tumor model.

Results USP2 expression was suppressed in cisplatin-resistant NSCLC cells. USP2 overexpression inhibited cell viability in cisplatin-resistant cells. Among the ferroptosis markers, the results showed that USP2 overexpression promoted LDH release, Fe²⁺ level, MDA and Lipid ROS, while inhibited GPX4 activity and GSH levels. The WB results revealed that USP2 overexpression inhibited GPX4, SLC7A11 and cytoplasm p53 protein expression, while promoted the nucleus p53 protein expression. Moreover, USP2 directly bound to p53 and USP2 overexpression stabilized p53 protein by suppressing its ubiquitination. In vivo experiments further suggest that the USP2-p53 pathway plays a crucial role in regulating cisplatin sensitivity in A549/DDP cells.

Conclusion USP2 acted on the K305R site of p53, which resulted in its deubiquitination. This cellular process could modulate cisplatin resistance through ferroptosis in NSCLC. This study could provide a potential therapeutic target to NSCLC.

Keywords USP2, p53, Cisplatin resistance, Ferroptosis

*Correspondence:

Li Jia
jjiali202311@163.com

¹Department of Oncology, Yuncheng Central Hospital Affiliated to Shanxi Medical University, Yuncheng 044000, Shanxi, China



© The Author(s) 2025. **Open Access** This article is licensed under a Creative Commons Attribution-NonCommercial-NoDerivatives 4.0 International License, which permits any non-commercial use, sharing, distribution and reproduction in any medium or format, as long as you give appropriate credit to the original author(s) and the source, provide a link to the Creative Commons licence, and indicate if you modified the licensed material. You do not have permission under this licence to share adapted material derived from this article or parts of it. The images or other third party material in this article are included in the article's Creative Commons licence, unless indicated otherwise in a credit line to the material. If material is not included in the article's Creative Commons licence and your intended use is not permitted by statutory regulation or exceeds the permitted use, you will need to obtain permission directly from the copyright holder. To view a copy of this licence, visit <http://creativecommons.org/licenses/by-nc-nd/4.0/>.

Introduction

Non-small cell lung cancer (NSCLC) is a common malignancy, which accounts for 85% lung cancer cases [1]. Recently, significant progresses have been made in the NSCLC treatment, specifically with the introduction of immunotherapy, however, cisplatin-based chemotherapy remains the primary treatment modality [2, 3]. Unfortunately, many patients eventually acquire cisplatin resistance, resulting in a decline in treatment efficacy or poor prognosis [4]. Therefore, it is crucial for NSCLC treatment to understand the molecular mechanisms of cisplatin resistance and identify novel effective biomarkers.

Tumor cells frequently display impairments programmed cell death mechanism, which primarily contributes to treatment failure and drug resistance. Meanwhile, to fulfill their growth demands, tumor cells require more iron, which render tumor more vulnerable to ferroptosis [5]. Ferroptosis differs from conventional necrosis, apoptosis, and autophagy in terms of morphology, biochemistry, and genetics. It exerts critical regulatory functions in tumor progression, rendering it potential candidate for cancer treatment [6]. Recent studies have revealed that inhibitory of ferroptosis is the main cause of drug chemotherapy resistance and the modulation of ferroptosis has been proved to reduce chemotherapy resistance [7]. However, the specific underlying mechanisms still are unknown and require further investigation.

The p53 tumor suppressor is crucial for normal cell growth and tumor prevention [5]. Mutations in p53 are found in most human cancers, not only impairing its anti-tumor activity but also acquiring oncogenic properties [8]. Tumors with mutated p53 typically progress faster and respond poorly to anti-cancer treatments with a poor prognosis [9]. Moreover, previous studies have identified the involvement of p53 in ferroptosis [10]. In terms of ferroptosis, p53 could inhibit SLC7A11 expression to suppress the synthesis of glutathione (GSH), ultimately inducing ferroptosis [11]. Additionally, p53 could also induce ferroptosis through SAT1/ ALOX15 axis in cancer cells [12]. In summary, p53 could inhibit tumor development by promoting cellular ferroptosis. However, the upstream target regulation of p53 remains unclear and further research is required.

Previous study has confirmed the ubiquitin-proteasome system (UPS) as cancer treatment strategies [13]. The UPS is an essential protein degradation route in living organisms, consisting of ubiquitin, ubiquitin-conjugating enzymes, and the 26 S proteasome. This system mediates the degradation of proteins by ubiquitinating target proteins and sending them to the proteasome complex for degradation, thereby regulating many cellular processes including cell cycle [14], apoptosis [15], immune response [16]. USP2 exhibits dual effects in cancer, acting both as an oncogene and a tumor suppressor.

It is upregulated in various malignancies, such as triple negative breast cancer [17] and choroidal melanoma [18] and USP2 overexpression stimulates cell migration and invasion. Conversely, USP2 inhibits glioblastoma development by suppressing the TGF- β signaling pathway through the deubiquitination of SMAD7 [19]. Furthermore, USP2 suppresses lung cancer progression through reducing the ubiquitin-mediated decrease of the ARID2 protein [20]. However, recent research has revealed the correlation between USP and drug resistance, for instance, in gastric cancer, USP7 is overexpressed and deubiquitinates hnRNPA1, which ultimately promotes the cisplatin resistance in gastric cancer cells [21]. USP22 expression is upregulated and its overexpression promotes cisplatin resistance by enhancing their DNA repair capability in drug-resistant lung adenocarcinoma [22]. However, further investigation is warranted to elucidate the underlying mechanism of cisplatin resistance by USP2 in NSCLC.

In our study, we investigated the expression of USP2 in DDP-resistant NSCLC cells and found that USP2 expression was inhibited in these cells. Further research revealed that USP2 overexpression suppressed cell viability in DDP-resistant NSCLC and promoted ferroptosis. Additionally, we discovered that USP2 facilitated the nuclear translocation of p53, a process mediated by the regulation of p53 ubiquitination. Our study preliminarily unveils a novel mechanism of DDP resistance in NSCLC, highlighting the critical role of the USP2-p53 axis in regulating cisplatin sensitivity in NSCLC cells.

Materials and methods

Cell culture and transfection

A549, A549/DDP, H1299 and H1299/DDP cells were procured from American Type Cell Collection. A549/DDP and H1299/DDP with K305R, K372R, and K382R mutations were obtained from Cyagen Biosciences (China). McCoy's 5 A medium with the addition of 1% penicillin streptomycin and 10% FBS supplementation was utilized for cell culture. Moreover, the McCoy's 5 A medium used for cisplatin-resistant cells culturation contained 1 μ M cisplatin. Subsequently, the short hairpin RNA targeted to USP2 (sh-USP2), the pLVX-IRES-ZsGreen vector carrying USP2 sequences and corresponding controls (sh-NC and vector) was transfected into the cisplatin-resistant cells lines through Lipofectamine 3000 (Invitrogen) separately. Puromycin and RT-qPCR were utilized for screening transfected cells and verify transfection efficiency. All cells were incubated at 37 °C in an incubator supplied with 5% CO₂.

Cell counting Kit-8 (CCK-8) and IC50 assays

CCK-8 (Thermo Fisher, USA) was utilized for cell viability detection. Approximately 10³ cells were incubated

for 1 day in 96-well plates. After incubation with CCK-8 reagent, optical density (OD) values were determined through microplate reader at 450 nm. For IC50 assays, cells were exposed to cisplatin for 2-day incubation (0.1, 1, 10 and 100 µg/mL). Finally, IC50 values were calculated based on the cell viability results.

RT-qPCR

RNA isolation was performed using Trizol (Takara). The quantity and purity of RNA were determined spectrophotometrically through NanoDrop 2000 instrument (Thermo Fisher, USA). PrimeScript RT-PCR kit (Takara) and SYBR Premix Ex Taq (Takara) were utilized for cDNA generation and measurement according to the instruction of manufacturer. Expression levels were normalized to GAPDH as an internal reference using the $2^{-\Delta\Delta Ct}$ method.

Lactate dehydrogenase (LDH)

The cell LDH activity was assessed utilizing LDH Cytotoxicity Assay Kit (Glpbio, USA). To prepare sample, cells were lysed and the supernatant was extracted. Then, 120 µL supernatant was mixed with 60 mL LDH reagent and incubated for 30 min. Subsequently, OD values of the reaction mixture were detected at 490 nm through spectrophotometer. The LDH standard reagent (0, 10, 20, 30, 40, 50 U/L) was utilized to make standard curves. Finally, the LDH activity was calculated according to the standard curves.

GSH measurement

Glutathione peroxidase assay kit (Abcam, ab102530) was utilized to measure GSH activity. Cells were lysated with 200 µL lysis buffer; the mixture was centrifuged at 12,000 rpm for 10 min at 4 °C. The supernatant was then combined with glutathione peroxidase detection buffer and GPX detection working solution with 15-min incubation at room temperature. Subsequently, peroxide reagent solution was added and thorough mixed. Absorbance was detected at 340 nm through a spectrophotometer to determine GSH activity.

GPX4 enzyme activity

Phospholipid hydroperoxide glutathione peroxidase, mitochondrial (GPX4) ELISA Kit (Avantor) was utilized for GPX4 enzyme activity measurement. Cell lysates was added into each well and incubated at 37 °C for 80 min. The solution was discarded, and the plate was washed with washing buffer to remove any unbound materials. After drying, 100 µL biotinylated antibody working solution was added and incubated for 50 min at 37 °C. The solution was discarded and the plate was washed. After drying, 100 µL HRP enzyme working solution was added and incubated for 50 min at 37 °C. The solution

was discarded, and the plate was washed to completely remove any unbound materials. After drying, 90 µL TMB substrate was added and incubated for 20 min at 37 °C. Subsequently, 50 µL stop solution was added with immediate measurement at 450 nm. Based on the absorbance values, the activity of GPX4 enzyme was calculated.

Malondialdehyde (MDA)

Malondialdehyde Colorimetric Assay Kit (Thermo Fisher, USA) was utilized for cellular MDA measurement. Cells were cultured, harvested, lysed, and protein concentration was quantified. Then, the lysate was combined with MDA working solution, heated in a water bath at 100 °C for 15 min, centrifuged at 12,000 rpm for 15 min, and the supernatant was measured spectrophotometrically at 532 nm. Finally, cell MDA activity was calculated based on OD values.

Lipid reactive oxygen species (ROS)

BODIPY™ 581/591 C11 (Thermo Fisher, USA) was utilized for Lipid ROS detection. Approximately 10^6 cells were cultured in the medium for 30 min, which contained 10 µM BODIPY™ 581/591 C11. The trypsin with no EDTA was utilized for cell collection. Then, cells were washed twice following suspension in PBS. CytoFLEX cytometer instrument (Beckman Coulter) was utilized for Lipid ROS detection.

Extraction of nuclear and cytoplasmic proteins

Nuclear Protein Extraction Kit (abcam, ab113474) was utilized for nuclear and cytoplasmic proteins extraction. 200 µL cell protein extraction reagent was added into 10^6 cells and they were vigorously vortexed for 20 s to form a single-cell suspension. The mixture was placed in an ice bath for 10 min, followed by another 20-second vortex at 4 °C and centrifugation at 16,000 rpm for 10 min. The supernatant obtained after centrifugation represents the extracted cell cytoplasmic protein, while the precipitate represents the cell nucleus. The supernatant was removed and 100 µL nuclear protein extraction reagent was added, followed by another 20-second vortex to disperse the precipitate. The mixture was then placed in an ice-water bath for 10 min, followed by another 20-second vortex at 4 °C and centrifugation at 16,000 rpm for 10 min. The supernatant was the cell nuclear protein.

Fluorescence in situ hybridization (FISH)

The subcellular localization of p53 was tested by FISH. Oligonucleotide modified probes labeled with FAM for p53 was provided by GenePharma Co. The transfected A549/DDP and H1299/DDP cells were fixed in 4% formaldehyde (Beyotime, China) for 10 min and then treated with pre-hybridization buffer overnight at 37 °C. Following this, the cells were dyed with DAPI working solution.

Finally, images were taken using a laser confocal fluorescence microscope.

For tumor tissues, paraffin sections were hybridized with the p53 probe and incubated overnight at 37 °C. DAPI was then used for nuclear counterstaining at room temperature. All fluorescence images were captured using a confocal laser microscope (Zeiss, Germany).

Western blotting

RIPA buffer and Bradford Protein Assay Kit (Thermo Fisher, USA) were utilized to extract protein and measure its concentration. Protein was separated through SDS-PAGE assay and blocked under non-fat milk. The membranes were incubated with primary antibodies for 24 h and secondary antibodies for 4 h. ECL chemiluminescent substrate and chemiluminescence imaging system were utilized for bands visualization. Primary antibodies: Anti-USP2 antibody (ab168945), Anti-USP7 antibody (ab190183), Anti-USP11 antibody (ab109232), Anti-USP24 antibody (ab129064), Anti-USP37 antibody (ab72199), Anti-USP50 antibody (ab170342), Anti-p53 antibody (ab32049), Anti-GPX4 antibody (ab125066), Anti-xCT antibody (ab307601), Anti-Transferrin Receptor antibody (ab109259), Anti-ACSL4 antibody (ab155282), Anti-GAPDH antibody (ab9485) and Anti-TBP antibody (#8515); Secondary antibodies: Goat Anti-Rabbit IgG H&L (ab6702).

Ubiquitination assay

Lysis buffer with protease inhibitors was utilized to lyse cells. p53 antibody-coated protein A/G agarose beads was utilized to extract p53 protein. SDS-PAGE and Western blotting were utilized for protein separation and ubiquitination detection. Primary antibodies: Anti-Ubiquitin antibody (ab140601); Secondary antibodies: Goat Anti-Mouse IgG H&L (HRP) (ab205719).

Co-immunoprecipitation

Cells were lysed with a lysis buffer containing protease inhibitors, and the supernatant was collected after centrifugation at 12,000 rpm for 10 min. p53 antibody-coated protein A/G agarose beads was utilized to extract target protein from the supernatant. After washing the beads with PBS, the elution buffer was used to elute the protein. Subsequently, western blotting was utilized for detecting the fluorescence signal of USP2.

Animal experimental assays

We selected SPF-grade male BALB/c nude mice aged 4–5 weeks to verify the effects of USP2 on the tumorigenicity of DDP-resistant A549/DDP cells and their impact on DDP resistance. A total of 4×10^6 A549/DDP cells with USP2 overexpression (USP2) and control (oe-NC) were injected subcutaneously into the right flank of the

nude mice. Seven days after inoculation, cisplatin (5 mg/kg, injected once every three days) or an equal volume of saline was administered via intraperitoneal injection. After 28 days, all mice were euthanized. The implanted tumors were excised and weighed. Tumor volume was calculated using the following formula: $(\text{length} \times \text{width}^2) / 2$. RT-qPCR and FISH experiments were conducted using the methods described above.

Statistical analysis

All data were expressed as mean \pm SD. Graphs were generated, and statistical analyses were performed using GraphPad Prism 8.0. The differences between two groups of data were tested using a student's t-test, and one-way ANOVA was used to analyze multiple groups. $P < 0.05$ indicated significant differences. Measurements were performed in triplicate for each sample to ensure reproducibility.

Results

USP2 expression was inhibited in cisplatin-resistant NSCLC cells

USP2 was significantly overexpressed in NSCLC, yet its function and associated mechanisms in cisplatin resistance remain unclear. We utilized A549/DDP and H1299/DDP cells primarily for investigating the molecular pathways of cisplatin resistance in NSCLC. Firstly, both normal and cisplatin-resistant NSCLC cells were treated with different doses of DDP (0.1, 1, 10, and 100 $\mu\text{g/mL}$), followed by the calculation of IC₅₀ values for each cell type using CCK-8 assays to assess cell viability. The findings revealed that both A549/DDP (Fig. 1A) and H1299/DDP (Fig. 1C) cell lines exhibited significant resistance to cisplatin when compared to their normal counterparts. The IC₅₀ values of A549/DDP and H1299/DDP were markedly elevated compared to the parental cell lines, reaching 30.09 $\mu\text{g/mL}$ (Fig. 1B) and 23.37 $\mu\text{g/mL}$ (Fig. 1D), respectively. These two cell lines were chosen for subsequent investigations. Previous study has hinted at a correlation between USP family and drug resistance, however, their potential role in NSCLC remained unclear. Therefore, we sought to explore this relationship further in NSCLC. We next examined the USP family members expression in normal and cisplatin-resistant NSCLC cells, including USP2, USP7, USP11, USP24, USP37 and USP50. It was observed that only USP2 mRNA and protein expression were reduced in both A549/DDP cells (Fig. 2A, C and D) and H1229/DDP (Fig. 2B, C and E) cells. Taken together, these results suggested that USP2 could be relative to cisplatin resistance of NSCLC cells.

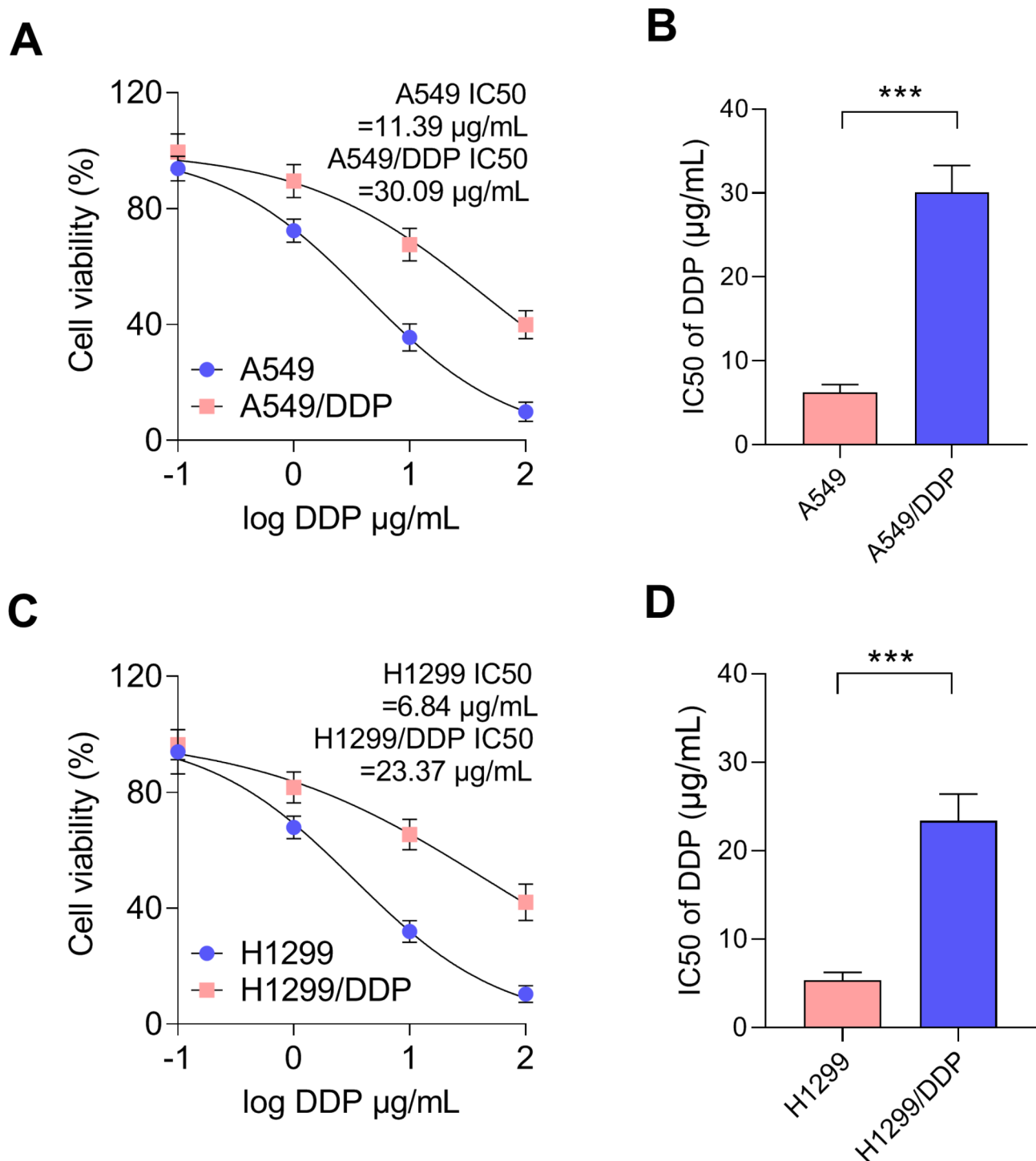


Fig. 1 A549/DDP and H1299/DDP cells showed increased resistance to DDP treatment. **(A)** The cell viability of A549 and A549/DDP cells was assessed through CCK-8 assays; **(B)** IC₅₀ of DDP in A549/DDP was assessed by CCK-8 assay. **(C)** The cell viability of H1299 and H1299/DDP cells was determined through CCK-8 assays. Cells were exposed to cisplatin (0.1, 1, 10, and 100 $\mu\text{g/mL}$) for 24 h. **(D)** IC₅₀ of DDP in H1299/DDP was assessed by CCK-8 assay. *** $p < 0.001$

USP2 overexpression inhibited cisplatin resistance through promoting ferroptosis in A549/DDP and H1299/DDP cells

Previous studies have identified differential expression of USP2. To systematically modulate USP2 expression

levels in drug-resistant cells, we employed cell transfection techniques. Specifically, the introduction of an overexpression vector for USP2 resulted in a significant increase in its expression (Fig. 2F). Conversely,

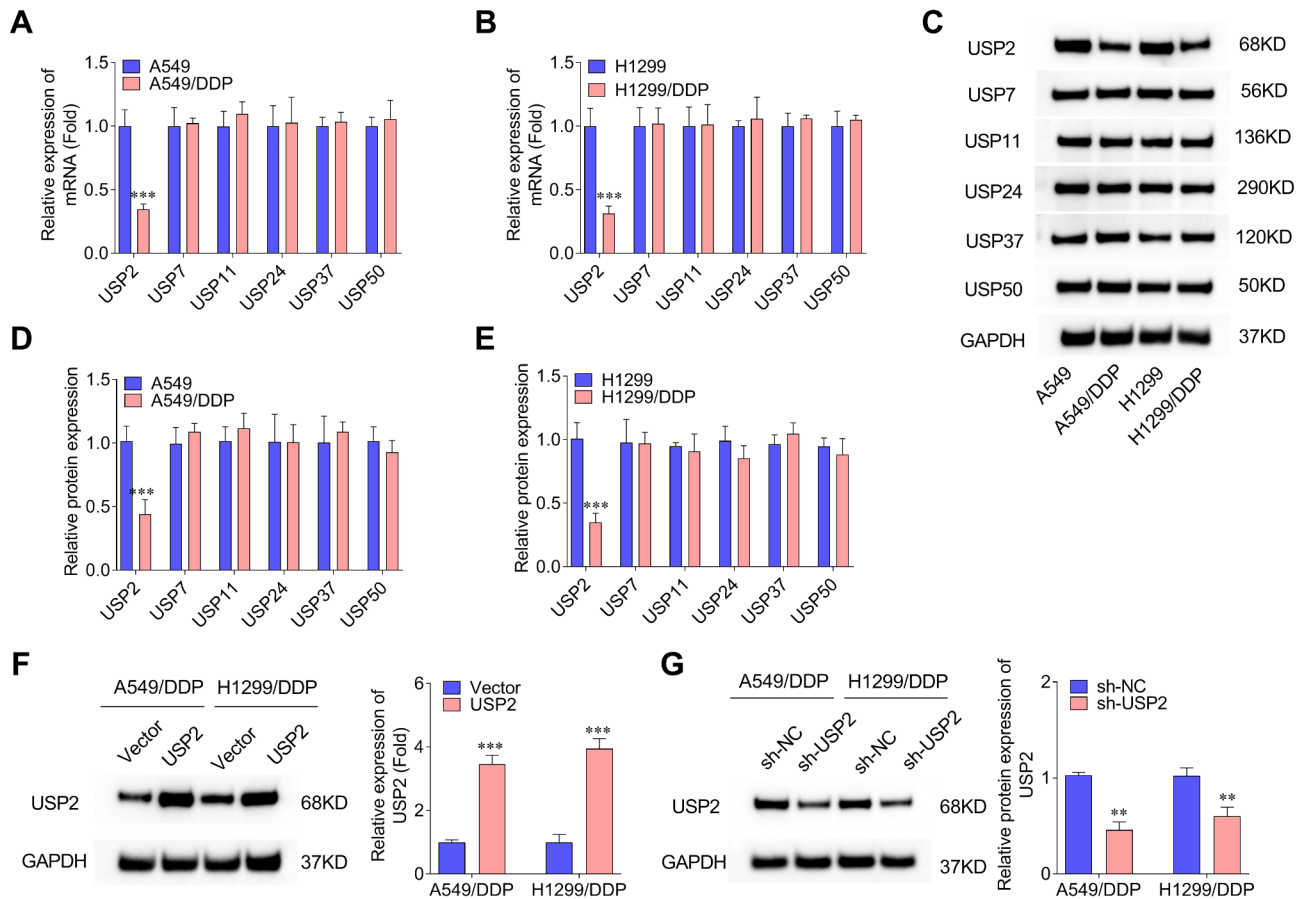


Fig. 2 USP2 expression was inhibited in A549/DDP and H1299/DDP cells. **(A)** RT-qPCR was utilized for assessing USP mRNA expression in A549 and A549/DDP cells; **(B)** The USP in H1299 and H1299/DDP cells was measured through RT-qPCR. **(C-E)** Western blotting was utilized for assessing USP protein expression in A549, A549/DDP, H1299 and H1299/DDP cells. **(F)** Western blotting and RT-qPCR was utilized for detecting the efficiency of silencing USP2. **(G)** Western blotting and RT-qPCR was utilized for detecting the efficiency of USP2 overexpression. ** $p < 0.01$, *** $p < 0.001$

transfection with sh-USP2 effectively decreased the expression of USP2 (Fig. 2G). Next, we investigated the effects of manipulating USP2 expression levels (either through knockdown or overexpression) on the cisplatin resistance of A549/DDP and H1299/DDP cells. Our findings demonstrated that USP2 overexpression notably suppressed cellular resistance, whereas USP2 knockdown enhanced the resistance of DDP-resistant cells (Fig. 3A and B). Considering the correlation between the reduced expression of USP2 in drug-resistant cells and the heightened drug resistance, we have chosen to center our forthcoming research on exploring the potential advantages of upregulating USP2. RT-qPCR was utilized to evaluate the transfection efficiency, which revealed a noteworthy overexpression of USP2 (Fig. 3C). Previous study has demonstrated that ferroptosis regulates cisplatin resistance in multiple cancers. To further investigate the potential involvement of USP2 in cisplatin resistance in NSCLC through ferroptosis, USP2 expression was overexpressed and the impact on cellular ferroptosis was assessed. Subsequently, CCK-8 assays were

utilized for measuring the cell viability in the presence of cisplatin (A549/DDP: 30.09 $\mu\text{g/mL}$, H1299/DDP: 23.37 $\mu\text{g/mL}$). The results indicated a notable suppression of cell viability in A549/DDP and H1299/DDP cells upon USP2 overexpression (Fig. 3D). Additionally, various marker of ferroptosis were assessed to investigate the impact of USP2. These markers included LDH, Fe^{2+} level, GPX4, GSH, MDA and Lipid ROS. The release of LDH into the medium occurs when the cell membrane is compromised. As expected, USP2 overexpression significantly intensified the cytotoxicity of cisplatin in NSCLC cells and resulted in increased LDH release (Fig. 3E). Moreover, USP2 overexpression promoted Fe^{2+} (Fig. 3F) levels in cisplatin-resistant cells. Notably, GPX4 and GSH metabolism play important functions in multiple cancers; their depletion induces ferroptosis accompanied by the accumulate of MDA and ROS. In our study, the overexpression of USP2 suppressed GPX4 activity (Fig. 3G) and GSH (Fig. 3H). A significant increase in MDA (Fig. 3I) and lipid ROS (Fig. 3J) was observed in the cisplatin-resistant cells. Our findings suggested that

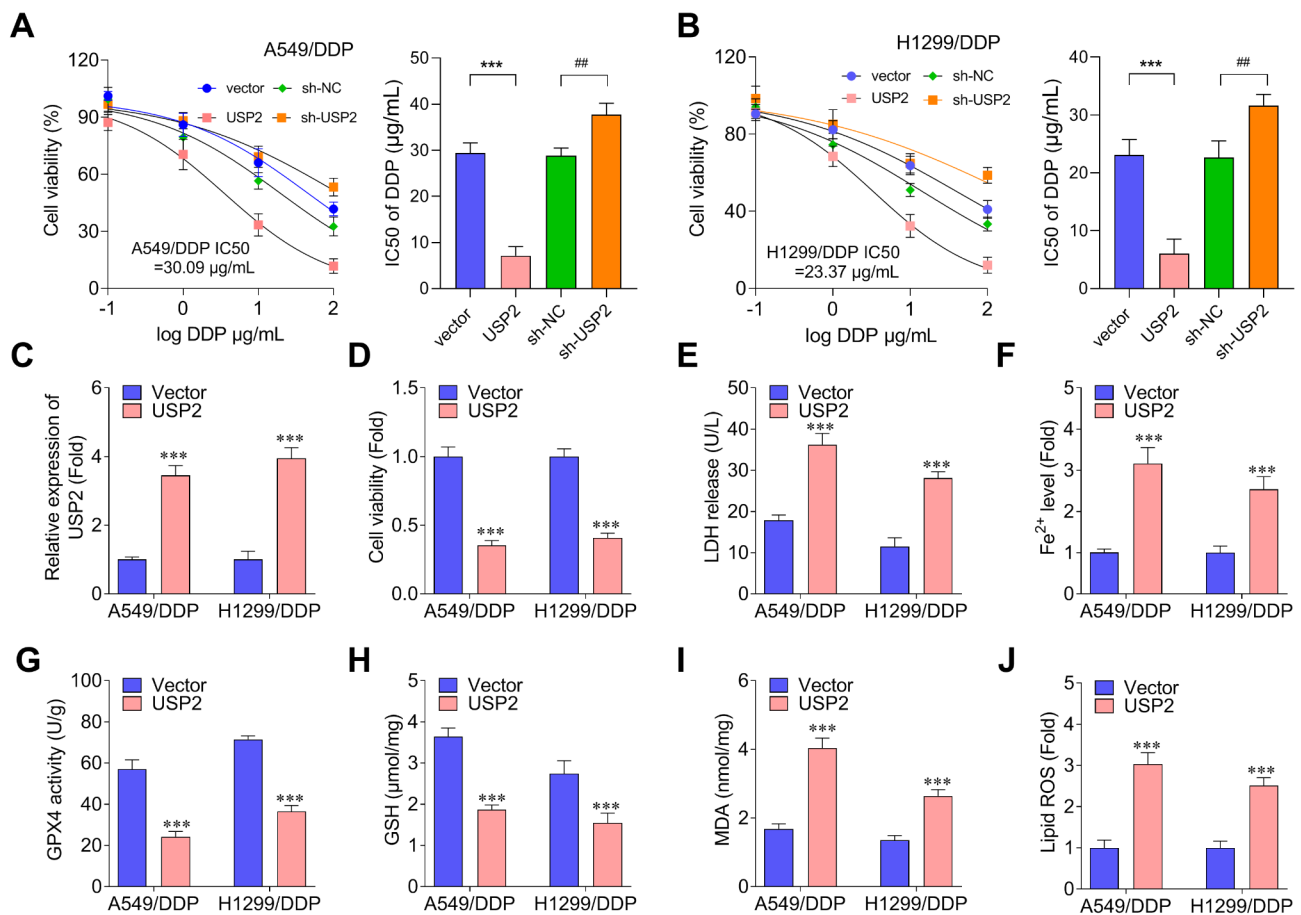


Fig. 3 USP2 promoted ferroptosis in A549/DDP and H1299/DDP cells. **(A)** The cell viability and IC₅₀ of A549 and A549/DDP cells was assessed through CCK-8 assays. **(B)** The cell viability and IC₅₀ of H1299 and H1299/DDP cells was assessed through CCK-8 assays. **(C)** RT-qPCR was utilized for detecting the efficiency of USP2 overexpression; **(D)** CCK-8 assays were utilized to measure the NSCLC cell viability exposed to cisplatin after USP2 overexpression; Ferroptosis markers, including LDH release **(E)**, Fe²⁺ level **(F)**, GPX4 **(G)**, GSH **(H)**, MDA **(I)** and lipid ROS **(J)**, were assessed after USP2 overexpression. ****p* < 0.001, ##*p* < 0.01

USP2 inhibited cisplatin resistance through promoting ferroptosis.

USP2 promoted ferroptosis through the nuclear transfer of p53

To explore the mechanism of USP2 and ferroptosis in NSCLC resistance to cisplatin, western blotting was utilized to measure the key protein markers of ferroptosis, including GPX4, SLC7A11, TFRC, and ACSL4. SLC7A11, a specific amino acid transporter, is a key regulatory protein of ferroptosis. Downregulation of SLC7A11 can lead to decreased intracellular cysteine levels and depletion of GSH biosynthesis by inhibiting cysteine metabolism, thereby indirectly inhibiting GPX4 activity and resulting in lipid peroxides accumulation, ultimately inducing ferroptosis [11]. In our study, USP2 overexpression significantly suppressed SLC7A11 and GPX4 expression (Fig. 4A, B and C). TFRC is a transferrin receptor, which regulates iron uptake; while ACSL4 is a key target of ferroptosis regulation, their inhibition can protect cells from

ferroptosis. However, we observed that USP2 overexpression had no effect on TFRC and ACSL4 protein expression. p53 is a substrate of USP2 and its accumulation in cells mediates various antitumor effects, such as DNA repair, apoptosis induction or cell cycle arrest. Additionally, recent research has reported that p53 is associated with cisplatin resistance in multiple cancer [23]. Therefore, we hypothesized that p53 may function in the NSCLC cisplatin resistance. Nevertheless, no significant difference was observed in the overall p53 protein expression. Subsequently, we separated the nucleus and cytoplasm, and evaluated their p53 protein expression independently. Notably, USP2 overexpression promoted p53 expression in the nucleus, while suppressing p53 expression in the cytoplasm (Fig. 4D). We speculate that the overexpression of USP2 promoted the nuclear translocation of p53. Through FISH experiments, we observed that following USP2 overexpression, the cytoplasmic level of p53 significantly decreased in H1299/DDP and A549/DDP cells, while its nuclear level significantly increased

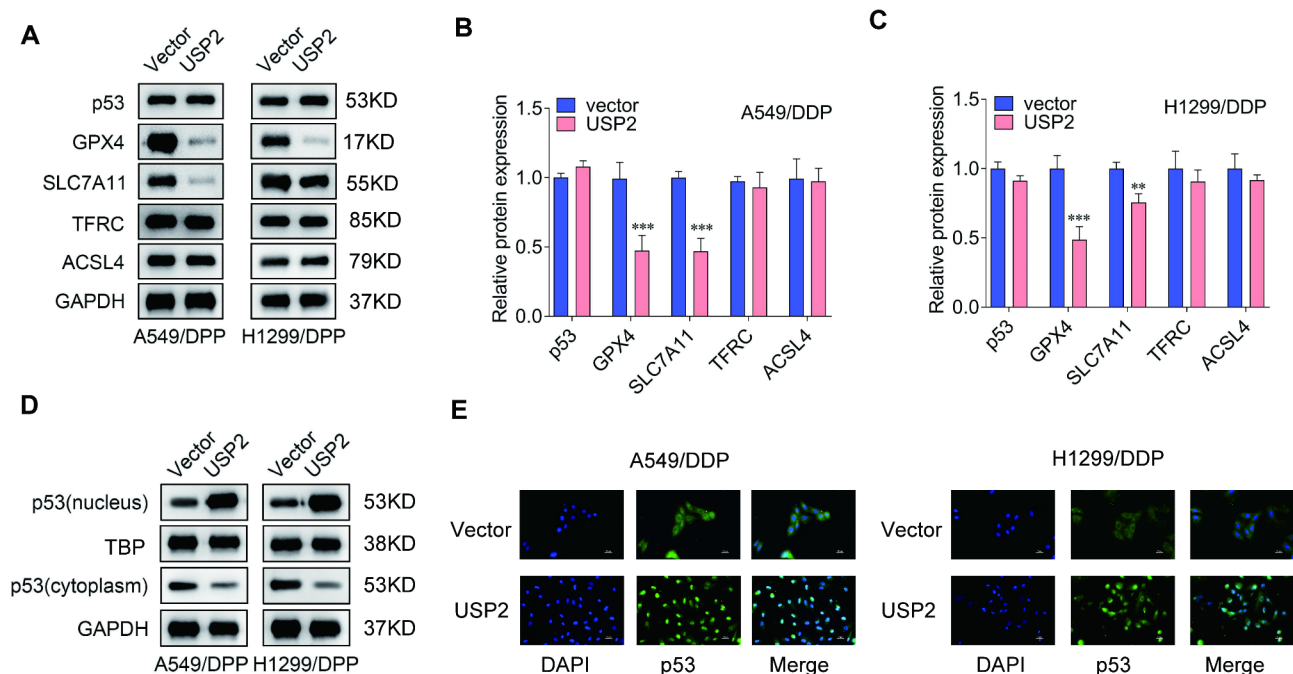


Fig. 4 USP2 promoted ferroptosis through the nuclear transfer of p53. **(A–C)** Western blotting was utilized for measuring p53 protein, GPX4, SLC7A11, TFRC and ACSL4 protein expression after USP2 overexpression. **(D)** Subcellular distribution of p53 expression in the nucleus and cytoplasm was assessed through western blotting after USP2 overexpression. **(E)** Localization of p53 in cells detected by fluorescence in situ hybridization (FISH) after USP2 overexpression. Scale bar = 10 μm. ** $p < 0.01$, *** $p < 0.001$

(Fig. 4E). This indicated that high USP2 expression facilitated p53 nuclear translocation in DDP-resistant NSCLC cells. Our findings suggest that USP2 promoted ferroptosis by enhancing the nuclear translocation of p53.

USP2 stabilized p53 protein by suppressing its ubiquitination

Ubiquitination marks proteins for degradation by proteasome, which affects their localization, activity and protein interactions [24]. To elucidate whether USP2 regulates cisplatin resistance through p53 ubiquitination, ubiquitination assays were utilized to assess p53 ubiquitination levels after USP2 overexpression. The results demonstrated that USP2 overexpression significantly inhibited p53 ubiquitination levels (Fig. 5A). Subsequently, COIP was utilized to identify the binding of USP2 and p53, which showed the direct binding between USP2 and p53 (Fig. 5B). Subsequently, to further explore the correlation between USP2 and p53 ubiquitination, we induced mutation at the K305R, K372R or K382R sites in cisplatin-resistant cells. The p53 ubiquitination levels was assessed, which indicated that K305R mutation significantly suppression p53 ubiquitination (Fig. 5C). Finally, nucleus and cytoplasm p53 protein expression was also evaluated. Interestingly, K305R mutation resulted in increased nuclear p53 expression and suppressed cytoplasmic p53 expression (Fig. 5D). Briefly, USP2 stabilized p53 protein by suppressing its ubiquitination and K305R site was the

potential target. In summary, USP2 acted on the K305R site of p53, which resulted in its deubiquitination. This cellular process could reduce cisplatin resistance through ferroptosis in NSCLC.

USP2 enhanced A549/DDP cells to cisplatin sensitivity in vivo

Subsequently, in vivo experiments were conducted using mice to further investigate the effect of USP2 on DDP resistance in A549/DDP cells. As illustrated in Fig. 6A–C, the combination of USP2 overexpression and DDP treatment promoted tumor regression, evidenced by a significant reduction in tumor volume and notable decrease in weight. This finding was consistent with the results from the in vitro functional assays. Furthermore, assessment of tissues USP2 revealed that overexpression of USP2 enhanced its expression in mice tissues (Fig. 6D). To determine the expression and localization of p53, we performed FISH experiments on mouse tissues. The results indicated that USP2 overexpression facilitated the nuclear expression of green fluorescence of p53 (Fig. 6E). These findings further suggest that the USP2-p53 pathway played a crucial role in regulating cisplatin sensitivity in A549/DDP cells.

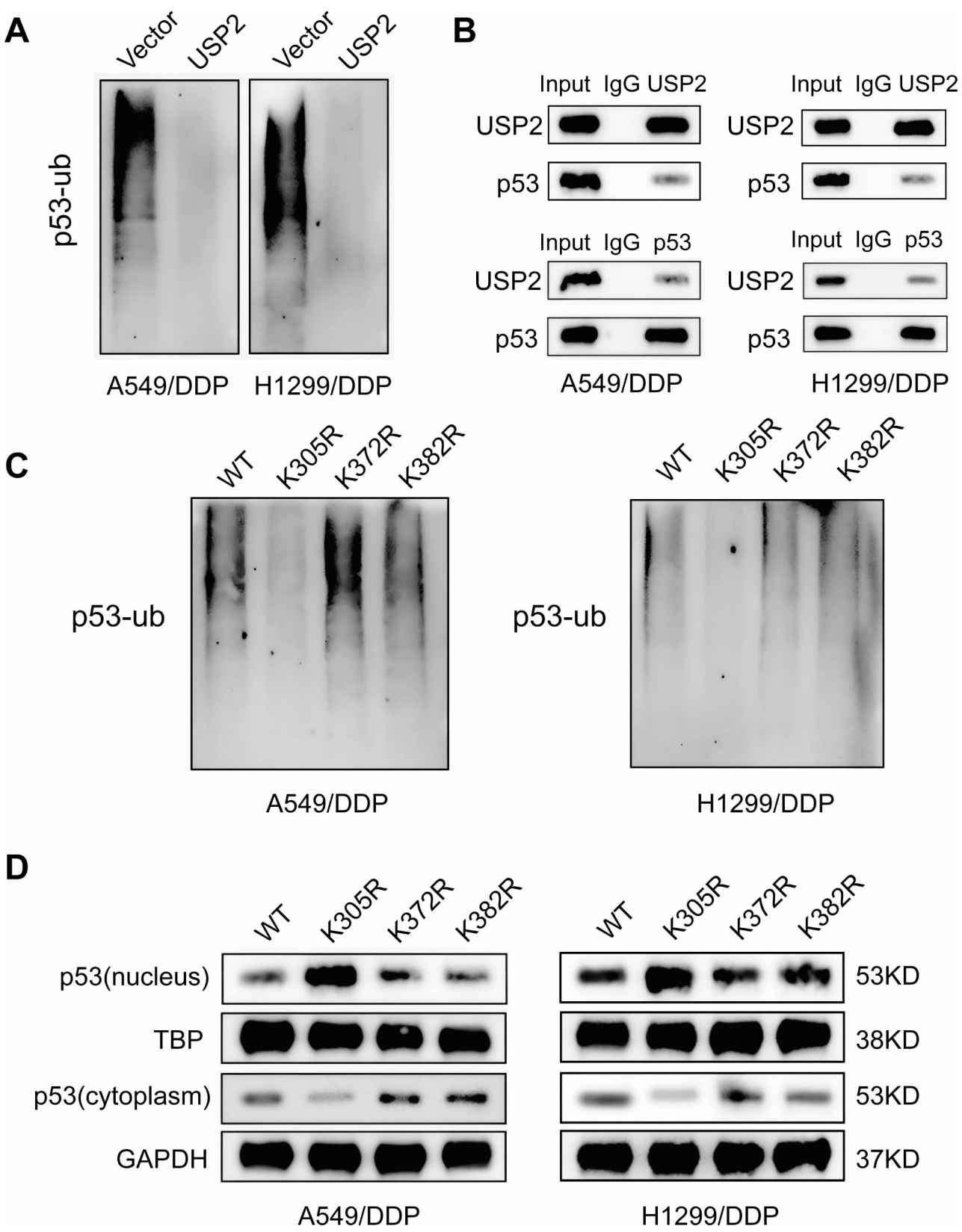


Fig. 5 USP2 stabilized p53 protein by suppressing its ubiquitination. **(A)** Ubiquitination Assay was utilized to measure p53 ubiquitination after USP2 overexpression. **(B)** COIP was utilized to detect the binding relationship of USP2 and p53. **(C)** The p53 ubiquitination levels were assessed after mutation at the K305R, K372R or K382R sites in A549/DDP and H1299/DDP cells. **(D)** Western blotting was utilized for detecting the nucleus and cytoplasm p53 expression after mutation at the K305R, K372R or K382R sites in A549/DDP and H1299/DDP cells

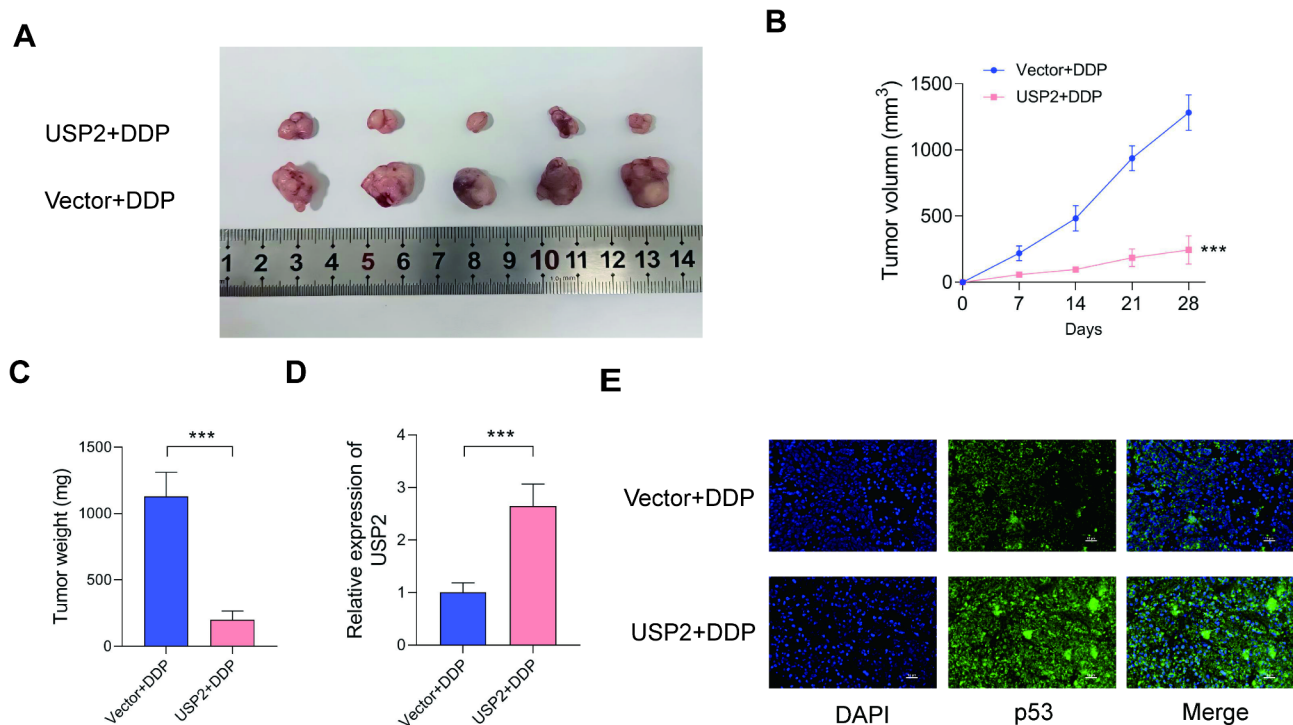


Fig. 6 USP2 overexpression enhanced DDP sensitivity in vivo. **(A)** Images of mice tumors after dissection. **(B)** Tumor volume in different treatment groups of mice was monitored every week. **(C)** Weights of dissected tumors in different treatment groups of mice. **(D)** The expression levels of USP2 were measured through RT-qPCR. **(E)** Localization of p53 in tissues detected by FISH in different treatment groups of mice. Scale bar = 10 μ m. $n=5$ biological samples, *** $p<0.001$

Discussion

NSCLC is the worldwide common and serious cancer. In recent years, significant breakthroughs have been made in NSCLC treatment with continuous research. However, the cisplatin resistance remains the major obstacle to chemotherapy in NSCLC [25]. The cancer resistance ultimately results in the failure of chemotherapy accompanied with an increase of mortality rates [26]. Consequently, it is imperative to elucidate the molecular mechanisms of cisplatin resistance in NSCLC. Our study revealed the function of USP2 on cisplatin resistance in NSCLC. Interestingly, USP2 expression was inhibited in A549/DDP and H1299/DDP cells compared to their normal counterparts. Moreover, USP2 overexpression could promote ferroptosis through p53 deubiquitination. Overall, USP2 inhibited cisplatin resistance through promoting ferroptosis in NSCLC.

USP2, a deubiquitinating enzyme, performs crucial biological functions related to ubiquitination. Previous research has primarily centered on the functions of USP2 in the development and progression of various cancers, including bladder cancer [27], breast cancer [28], and colon cancer [29]. It has established that USP2 functions as a tumor suppressor in numerous malignancies through multiple mechanisms; for instance, USP2 deubiquitinates SMAD7 and suppresses TGF- β signaling pathway

to inhibit glioblastoma progression [19]. Additionally, USP2 inhibits lung cancer through ubiquitinating ARID2 protein [20]. Recent studies revealed that UPS might be involved in cancer drug resistance and sensitivity. For example, USP8 is elevated in cisplatin-resistant ovarian cancer cells; silencing USP8 could sensitize ovarian cancer to cisplatin treatment, leading to improved chemotherapy outcomes [30]. USP14 expression is inhibited in ovarian cancer cisplatin resistant cells and its knockdown could decrease the cisplatin cytotoxicity [31]. Additionally, it is observed that USP1 inhibition could revert cisplatin resistance in NSCLC [32]. Our study discovered that USP2 seemed to act as a drug sensitivity modulator. The USP2 expression was downregulated in A549/DDP and H1299/DDP cells; its overexpression resulted in reduced cell viability of cisplatin-resistant NSCLC cells exposed to cisplatin.

Additionally, ferroptosis, a programmed cell death, is induced with the ROS accumulation, particularly lipid ROS [33]. glutathione peroxidase (GPX4) performs important functions in regulating cell ferroptosis in various cancers as antioxidant defense enzyme. Briefly, suppression of GPX4 promotes ferroptosis and the overexpression of GPX4 inhibits ferroptosis in multiple cancers. GPX4 could eliminate lipid peroxidation at the cost of GSH [34]. Subsequently, the depletion of GSH results

in lipid peroxidation, which effectively induces ferroptosis. The essence of ferroptosis is the glutathione depletion, the reduction of GPX4 activity and the failure of lipid oxides to be metabolized through the glutathione reductase reaction catalyzed by GPX4 [35]. Moreover, divalent iron ions oxidize lipids, leading to the generation of reactive oxygen species and ultimately promoting cellular ferroptosis. In general, ferroptosis occurrence is accompanied with the augmentation in LDH, MDA, lipid ROS and Fe^{2+} levels. Considerable clinical investigations have identified a correlation between ferroptosis and drug resistance [36]. In summary, the induction of ferroptosis has been established as an efficacious strategy for promoting drug sensibility formation, whereas the inhibition of ferroptosis exacerbates the formation of drug resistance [7]. Moreover, UPS orchestrates ferroptosis by the iron and lipid peroxidation accumulation, such as USP7 [37], USP8 [38] and USP35 [39]. Therefore, we hypothesized that USP2 might inhibit cisplatin resistance of NSCLC cells through promoting ferroptosis. To verify this speculation, we overexpressed USP2 expression and measured the cellular ferroptosis levels. As anticipated, USP2 overexpression promoted LDH release, Fe^{2+} level, MDA and lipid ROS, while inhibited GPX4, GSH and SLC7A11 levels. The evidence suggested that USP2 overexpression promoted ferroptosis in NSCLC cells.

Moreover, p53 is also involved in regulating ferroptosis [10–12]. However, p53 is an unstable protein in cells due to the presence of MDM2 proteins, which could ubiquitinate p53 to facilitate its degradation or directly bind to p53 to inhibit its transcriptional activation function [40]. Once cells are stimulated, the binding between MDM2 and p53 is disrupted, resulting in p53 protein accumulation, which enables cells to respond to stimulus. Briefly, to exert its tumor suppressor function, p53 needs to escape MDM2-mediated degradation and stabilize p53 protein to exert its function [41]. Previous study has also confirmed that USP protein family plays crucial functions in p53 escaping MDM2-mediated degradation. For instance, the deubiquitinases, such as USP2 [42], USP7 [43], and USP8 [44], exhibit potent deubiquitinating activity, resulting in the suppression of p53 ubiquitination and the consequent manifestation of their anticancer properties. However, it has been observed that the upregulation of USP2a promotes the accumulation of MDM2, MDM2-mediated ubiquitination, and p53 degradation [45]. More Intriguingly, studies conducted by Gu Wei have unveiled that during tumor suppression, despite the occurrence of p53 activation in murine models, there seems to be no noticeable escalation in the abundance of p53 protein. This observation suggests that p53 activation may not necessarily hinge on an increase in its protein levels, but rather on the relief of inhibitory effects mediated through transcriptional repression

proteins [12]. Furthermore, it has been also found that USP10 enhances the stability of p53 by deubiquitinating it and promotes the translocation of p53 from the cytoplasm to the nucleus [46]. In our study, USP2 overexpression inhibited p53 ubiquitination and directly interacted with p53. Additionally, the mutation of K305R site significantly reduced the ubiquitination levels of p53 and facilitated its translocation from the cytoplasm to the nucleus. Therefore, we speculate that USP2 overexpression may lower the ubiquitination levels of p53 by acting on the K305R site of p53 protein and promote the translocation of p53 from the cytoplasm to the nucleus. However, further research is required to confirm this hypothesis.

In vivo experiments in mice further confirmed that USP2 played a key role in regulating DDP sensitivity and p53 expression in tumor tissues. Although this study provides a preliminary exploration of the role of the USP2-p53 axis-mediated ferroptosis in reversing cisplatin resistance in NSCLC, several limitations persist. This research involved only two representative resistant cell lines, A549/DDP and H1299/DDP, indicating a need for future studies to broaden the range of cell lines used. Additionally, this study was conducted solely in vivo in mice, lacking relevant clinical data. Therefore, future research should urgently focus on expanding the sample size and variety, not only validating the findings in additional resistant cell lines but also incorporating more clinical data for thorough validation. Furthermore, future studies should focus on exploring the complex regulatory networks downstream of this axis to provide insights for developing novel therapeutic strategies.

Conclusions

This study revealed that USP2 and p53 were associated with NSCLC cisplatin resistance. Mechanistically, USP2 acted on the K305R site of p53, which resulted in its deubiquitination. This cellular process could modulate cisplatin resistance through ferroptosis in NSCLC. Therefore, targeting USP2/p53 axis could have promising therapeutic implications for NSCLC treatment.

Abbreviations

NSCLC	Non-small cell lung cancer
USP	Ubiquitin-specific protease
LDH	Lactate dehydrogenase
WB	Western blotting
Co-IP	Co-Immunoprecipitation
GSH	Synthesis of glutathione
CCK-8	Cell Counting Kit-8
OD	Optical density
MDA	Malondialdehyde
ROS	Reactive oxygen species
FISH	Fluorescence in situ hybridization

Supplementary Information

The online version contains supplementary material available at <https://doi.org/10.1186/s12920-025-02108-5>.

Supplementary Material 1

Acknowledgements

Not applicable.

Author contributions

Y.G. designed the study, performed the experiments, and drafted the manuscript. R.L. collected data, processed statistical data, and performed the experiments. R.Z. analyzed and interpreted the data. L.J. designed, supervised the study, and revised the manuscript. All authors read and approved the final version of the manuscript.

Funding

Not applicable.

Data availability

Data used to support the findings of this study are available from the corresponding author upon request.

Declarations**Ethics approval and consent to participate**

Not applicable.

Consent for publication

Not applicable.

Competing interests

The authors declare no competing interests.

Received: 13 November 2024 / Accepted: 17 February 2025

Published online: 26 February 2025

References

1. Suster DI, Mino-Kenudson M. Molecular Pathology of primary non-small cell Lung Cancer. *Arch Med Res*. 2020;51(8):784–98.
2. Tang S, Qin C, Hu H, Liu T, He Y, Guo H et al. Immune checkpoint inhibitors in Non-small Cell Lung Cancer: Progress, challenges, and prospects. *Cells*. 2022;11(3).
3. Chaft JE, Shyr Y, Sepesi B, Forde PM. Preoperative and postoperative systemic therapy for operable non-small-cell Lung Cancer. *J Clin Oncol*. 2022;40(6):546–55.
4. Xie H, Yao J, Wang Y, Ni B. Exosome-transmitted circVMP1 facilitates the progression and cisplatin resistance of non-small cell lung cancer by targeting miR-524-5p-METTL3/SOX2 axis. *Drug Deliv*. 2022;29(1):1257–71.
5. Hassannia B, Vandenabeele P, Vanden Berghe T. Targeting ferroptosis to Iron Out Cancer. *Cancer Cell*. 2019;35(6):830–49.
6. Kim R, Hashimoto A, Markosyan N, Tyurin VA, Tyurina YY, Kar G, et al. Ferroptosis of tumour neutrophils causes immune suppression in cancer. *Nature*. 2022;612(7939):338–46.
7. Zhang C, Liu X, Jin S, Chen Y, Guo R. Ferroptosis in cancer therapy: a novel approach to reversing drug resistance. *Mol Cancer*. 2022;21(1):47.
8. Liu H, Lan T, Li H, Xu L, Chen X, Liao H, et al. Circular RNA circDLC1 inhibits MMP1-mediated liver cancer progression via interaction with HuR. *Theranostics*. 2021;11(3):1396–411.
9. Zhou X, Hao Q, Lu H. Mutant p53 in cancer therapy-the barrier or the path. *J Mol Cell Biol*. 2019;11(4):293–305.
10. Mustafa Rizvi SH, Shao D, Tsukahara Y, Pimentel DR, Weisbrod RM, Hamburg NM, et al. Oxidized GAPDH transfers S-glutathionylation to a nuclear protein Sirtuin-1 leading to apoptosis. *Free Radic Biol Med*. 2021;174:73–83.
11. Zeng C, Lin J, Zhang K, Ou H, Shen K, Liu Q, et al. SHARPIN promotes cell proliferation of cholangiocarcinoma and inhibits ferroptosis via p53/SLC7A11/GPX4 signaling. *Cancer Sci*. 2022;113(11):3766–75.
12. Liu Y, Gu W. p53 in ferroptosis regulation: the new weapon for the old guardian. *Cell Death Differ*. 2022;29(5):895–910.
13. Park J, Cho J, Song EJ. Ubiquitin-proteasome system (UPS) as a target for anticancer treatment. *Arch Pharm Res*. 2020;43(11):1144–61.
14. Zhang Z, Chen J, Tang W, Feng Q, Xu J, Ren L. Comprehensive Analysis Reveals the potential Regulatory mechanism between Ub-Proteasome System and Cell Cycle in Colorectal Cancer. *Front Cell Dev Biol*. 2021;9:653528.
15. Abbas R, Larisch S. Killing by degradation: regulation of apoptosis by the ubiquitin-proteasome-system. *Cells*. 2021;10(12).
16. Çetin G, Klafack S, Studencka-Turski M, Krüger E, Ebstein F. The ubiquitin-proteasome system in Immune cells. *Biomolecules*. 2021;11(1).
17. Qu Q, Mao Y, Xiao G, Fei X, Wang J, Zhang Y, et al. USP2 promotes cell migration and invasion in triple negative breast cancer cell lines. *Tumour Biol*. 2015;36(7):5415–23.
18. Wei C, Zhao X, Zhang H, Wang L. USP2 promotes cell proliferation and metastasis in choroidal melanoma via stabilizing snail. *J Cancer Res Clin Oncol*. 2023;149(11):9263–76.
19. Tu Y, Xu L, Xu J, Bao Z, Tian W, Ye Y, et al. Loss of deubiquitylase USP2 triggers development of glioblastoma via TGF- β signaling. *Oncogene*. 2022;41(18):2597–608.
20. Zhu L, Chen Z, Guo T, Chen W, Zhao L, Guo L, et al. USP2 inhibits Lung Cancer Pathogenesis by reducing ARID2 protein degradation via Ubiquitination. *Biomed Res Int*. 2022;2022:1525216.
21. Zhang H, Deng T, Liu R, Ning T, Yang H, Liu D, et al. CAF secreted miR-522 suppresses ferroptosis and promotes acquired chemo-resistance in gastric cancer. *Mol Cancer*. 2020;19(1):43.
22. Guo J, Zhao J, Fu W, Xu Q, Huang D. Immune Evasion and Drug Resistance mediated by USP22 in Cancer: novel targets and mechanisms. *Front Immunol*. 2022;13:918314.
23. Jing X, Xie M, Ding K, Xu T, Fang Y, Ma P, et al. Exosome-transmitted mir-769-5p confers cisplatin resistance and progression in gastric cancer by targeting CASP9 and promoting the ubiquitination degradation of p53. *Clin Transl Med*. 2022;12(5):e780.
24. Mansour MA. Ubiquitination. Friend and foe in cancer. *Int J Biochem Cell Biol*. 2018;101:80–93.
25. Wang W, Zhao M, Cui L, Ren Y, Zhang J, Chen J, et al. Characterization of a novel HDAC/RXR/HtrA1 signaling axis as a novel target to overcome cisplatin resistance in human non-small cell lung cancer. *Mol Cancer*. 2020;19(1):134.
26. Teng X, Fan XF, Li Q, Liu S, Wu DY, Wang SY, et al. XPC inhibition rescues cisplatin resistance via the Akt/mTOR signaling pathway in A549/DDP lung adenocarcinoma cells. *Oncol Rep*. 2019;41(3):1875–82.
27. Liu XQ, Shao XR, Liu Y, Dong ZX, Chan SH, Shi YY, et al. Tight junction protein 1 promotes vasculature remodeling via regulating USP2/TWIST1 in bladder cancer. *Oncogene*. 2022;41(4):502–14.
28. Xu QT, Wang ZW, Cai MY, Wei JF, Ding Q. A novel cuproptosis-related prognostic 2-lncRNAs signature in breast cancer. *Front Pharmacol*. 2022;13:1115608.
29. Li D, Bao J, Yao J, Li J. lncRNA USP2-AS1 promotes colon cancer progression by modulating Hippo/YAP1 signaling. *Am J Transl Res*. 2020;12(9):5670–82.
30. Corno C, D'Arcy P, Bagnoli M, Paolini B, Costantino M, Carenini N, et al. The deubiquitinase USP8 regulates ovarian cancer cell response to cisplatin by suppressing apoptosis. *Front Cell Dev Biol*. 2022;10:1055067.
31. Luo H, Wang X, Ge H, Zheng N, Peng F, Fu Y, et al. Inhibition of ubiquitin-specific protease 14 promotes connexin 32 internalization and counteracts cisplatin cytotoxicity in human ovarian cancer cells. *Oncol Rep*. 2019;42(3):1237–47.
32. García-Santisteban I, Peters GJ, Giovannetti E, Rodríguez JA. USP1 deubiquitinase: cellular functions, regulatory mechanisms and emerging potential as target in cancer therapy. *Mol Cancer*. 2013;12:91.
33. Yuan Y, Zhai Y, Chen J, Xu X, Wang H. Kaempferol Ameliorates Oxygen-Glucose Deprivation/Reoxygenation-Induced Neuronal Ferroptosis by Activating Nrf2/SLC7A11/GPX4 Axis. *Biomolecules*. 2021;11(7).
34. Ursini F, Maiorino M. Lipid peroxidation and ferroptosis: the role of GSH and GPx4. *Free Radic Biol Med*. 2020;152:175–85.
35. Lei G, Zhuang L, Gan B. Targeting ferroptosis as a vulnerability in cancer. *Nat Rev Cancer*. 2022;22(7):381–96.
36. Fu D, Wang C, Yu L, Yu R. Induction of ferroptosis by ATF3 elevation alleviates cisplatin resistance in gastric cancer by restraining Nrf2/Keap1/xCT signaling. *Cell Mol Biol Lett*. 2021;26(1):26.
37. Tang LJ, Zhou YJ, Xiong XM, Li NS, Zhang JJ, Luo XJ, et al. Ubiquitin-specific protease 7 promotes ferroptosis via activation of the p53/TfR1 pathway in the rat hearts after ischemia/reperfusion. *Free Radic Biol Med*. 2021;162:339–52.
38. Liu L, Zheng B, Luo M, Du J, Yang F, Huang C, et al. Suppression of USP8 sensitizes cells to ferroptosis via SQSTM1/p62-mediated ferritinophagy. *Protein Cell*. 2023;14(3):230–4.

39. Tang Z, Jiang W, Mao M, Zhao J, Chen J, Cheng N. Deubiquitinase USP35 modulates ferroptosis in lung cancer via targeting ferroportin. *Clin Transl Med*. 2021;11(4):e390.
40. Zafar A, Wang W, Liu G, Xian W, McKeon F, Zhou J, et al. Targeting the p53-MDM2 pathway for neuroblastoma therapy: rays of hope. *Cancer Lett*. 2021;496:16–29.
41. Moll UM, Petrenko O. The MDM2-p53 interaction. *Mol Cancer Res*. 2003;1(14):1001–8.
42. Kitamura H, Hashimoto M. USP2-Related Cellular Signaling and Consequent Pathophysiological outcomes. *Int J Mol Sci* 2021;22(3).
43. Wang Z, Kang W, Li Q, Qi F, Wang J, You Y, et al. Abrogation of USP7 is an alternative strategy to downregulate PD-L1 and sensitize gastric cancer cells to T cells killing. *Acta Pharm Sin B*. 2021;11(3):694–707.
44. Sha B, Sun Y, Zhao S, Li M, Huang W, Li Z, et al. USP8 inhibitor-induced DNA damage activates cell cycle arrest, apoptosis, and autophagy in esophageal squamous cell carcinoma. *Cell Biol Toxicol*. 2023;39(5):2011–32.
45. Kim J, Keay SK, You S, Loda M, Freeman MR. A synthetic form of frizzled 8-associated antiproliferative factor enhances p53 stability through USP2a and MDM2. *PLoS ONE*. 2012;7(12):e50392.
46. Yuan J, Luo K, Zhang L, Cheville JC, Lou Z. USP10 regulates p53 localization and stability by deubiquitinating p53. *Cell*. 2010;140(3):384–96.

Publisher's note

Springer Nature remains neutral with regard to jurisdictional claims in published maps and institutional affiliations.